Article title: The roles of divergent and parallel selection in Amazonian and Andean bird responses to glacial cycles

Authors: Vanessa E. Luzuriaga-Aveiga[1,2]*, Matt J. Thorstensen[2]*, Jill E. Jankowski[3] & Jason T. Weir[1,2]

[1] Department of Ecology and Evolutionary Biology, University of Toronto, Toronto, ON, M5S 3B2, Canada

[2] Department of Biological Sciences, University of Toronto Scarborough, Toronto, ON, M1C 1A4, Canada

[3] Biodiversity Research Centre & Department of Zoology, University of British Columbia, Vancouver, BC, V6T 1Z4E, Canada

*Co-First Authors

Short running title: Parallel and divergent selection in birds

Keywords: Climatic cycle, species pair, Pleistocene, speciation, genomics, differentiation, richness, evolution

Number of words: Abstract: 150, main text: 4847

Number of references: 58

Number of figures: 4

Number of tables: 0

Corresponding author: Jason Weir. University of Toronto Scarborough, 1265 Military Trail, Toronto, Ontario, Canada M1C 1A4. Telephone: +1 (416) 208-5152, Fax: +1 (416) 287-7676, e-mail: jason.weir@utoronto.ca

Statement of authorship: VELA and JW conceived of and designed the study. JEJ and JW conducted field work. VELA performed lab work and bioinformatics. VELA, JW, and MJT conducted modeling. VELA, MJT, and JW wrote the first draft of the manuscript. All authors contributed substantially to revisions.

Data accessibility statement: Code and an example dataset of called SNPs for this work are provided on GitHub (https://github.com/Weir-Lab/sisterspecies_sweeps/). Raw sequencing reads are archived on the National Center for Biotechnology Information Sequence Read Archive (PRJNA665047, PRJNA600749, PRJNA433557, PRJNA421731, and PRJNA725153).

Abstract

Both divergent and parallel selection can contribute to evolutionary change, yet their relative contributions to adaptation and speciation are poorly understood, especially during environmental change. We quantified selective sweep signatures and divergence times in Amazonian avian sister species pairs that either differ in elevation and are expected to have experienced strong divergent selection; or occur in similar lowland habitats and are expected to have experienced strong parallel selection. We found that elevational differentiation resulted in a greater accumulation of selective sweep signatures over the five-million-year timespan covered by our dataset, supporting the importance of divergent selection. Nevertheless, lowland-restricted species pairs accumulated more selective sweeps over the most recent two million years, suggesting that parallel selection, driven by major Pleistocene glacial cycles, produced faster evolutionary change than divergent selection in elevationally differentiated species pairs. Our results highlight parallel selection as an important driver of adaptation and evolution, especially during environmental instability.

Introduction

Natural selection leading to adaptation is a fundamental force shaping genomic differentiation and biological diversity [1–5]. This genomic change may ultimately lead to the formation of new species due to the build-up of genetic incompatibilities that arise as closely related species differentially adapt [6,7]. Divergent natural selection, driven by environmental differences, can fast-track the formation of reproductive barriers between populations – a process often referred to as ecological speciation [8–10]. Populations can also differentiate under parallel selective forces when exposed to non-divergent environmental changes [11]. In this case, each population adapts to the same environmental changes but in different ways. This results in genomic differentiation that may lead to speciation, especially if adaptations are disrupted in hybrid individuals, in a process often referred to as mutation order speciation [12,13]. Despite divergent selection being a more studied and commonly proposed driver of trait evolution, recent comparative analyses across thousands of terrestrial vertebrate species suggested divergent selection drove differentiation in key ecological traits like body size and bill shape in only 10% of species [14]. These inconsistent findings demonstrate fundamental uncertainties about the roles of divergent versus parallel selection in adaptation and speciation.

The Amazon basin provides an ideal laboratory to investigate the roles of both divergent and parallel selection in evolution. Spanning more than six million square kilometers with an elevation range from near sea level to over six thousand meters along the eastern slope of the Andes, the Amazon basin harbors an extensive array of habitat types. Lowland rainforests are followed by the epiphyte encrusted subtropical montane forest zone at 1,300 to 2,400 meters, above which the temperate montane forest zone occurs to treeline (about 3,300 m), with paramo and puna grasslands above treeline [15] (Fig. 1). Many environmental factors vary with

elevation, including both climatic variables (e.g., precipitation, temperature, solar radiation, wind speed, oxygen pressure, atmospheric CO_2, etc.) and biotic factors (e.g., niche breadth, forest height, foraging strata, species diversity, competition strength, etc.) [16]. Moreover, glacial cycles influenced temperature and possibly rainfall across the Amazon basin. Elevational zones of the Andes shifted downslope during glacial periods. This environmental change over the past several million years was most heavily influenced by the mid-to-late Pleistocene glacial cycles [17–19]. However, unlike in northern latitudes, only the highest elevations of the Amazon basin in the high Andes were directly glaciated. While most Andean species may have simply tracked their preferred environmental conditions by moving downslope and upslope during and after glacial periods, lowland species, often surrounded by river barriers on multiple sides, had nowhere to migrate. Lowland populations may have been forced to adapt *in situ* to changing conditions.

These historical patterns of tracking elevation or adapting *in situ* may be evident in the population-level genomic variation of recently-diverged sister species pairs. Specifically, species pairs from different elevational zones would likely experience very different environmental pressures over time as species would first have had to adapt to different environments, then the lowland member of a pair would have continued to adapt to changing conditions over time while the highland member of a pair may have tracked its preferred habitat by migrating up- and down-slope during periods of warming or cooling. Conversely, species pairs with both members from the same elevational zone would have been lore likely to have experienced parallel environmental pressures during glacial cycles resulting in parallel selection as both species in a pair adapted to the same changes in climate [11]. Either circumstance of shared or different elevational zones between members of a sister species pair would have led to an accumulation of

96 selective sweeps after divergence [20], but the selective forces underlying such sweeps could be
97 either divergent or parallel. Therefore, we used species pairs with both members from the
98 lowlands to study parallel selection (acknowledging that some divergent selection may also
99 occur), and species pairs with members from the lowlands and highlands to study divergent
100 selection.

101 Here, we harness the power of genome-wide data to assess adaptation in closely related
102 pairs of avian species. Positive selection may produce selective sweeps in the genome where the
103 target of selection, and linked nearby regions, become fixed or highly differentiated between
104 populations (high fixation index, F_{ST}), while genetic diversity within populations (nucleotide
105 polymorphism, π) in these regions is reduced [21–23]. Genomic signatures of strong selective
106 sweeps often stand out as 'islands of differentiation' in F_{ST} and 'valleys of genetic diversity' in
107 π, relative to the genomic background signature of these metrics [20]. We calculated the number
108 of such regions in the genomes for a series of closely related species or genetically differentiated
109 populations within a species ("species pair" hereafter) (Fig. 2). To test the effect of elevational
110 differentiation on the accumulation of selective sweeps through time, we calculated divergence
111 time using site frequency spectrum-based demographic modelling [24]. Species pairs were
112 divided into two categories: lowland-restricted pairs, in which both species in a pair occur in the
113 lowlands of the Amazon (i.e., generally below 1000 m; n=9 pairs); and elevationally-
114 differentiated pairs, where the two species in each pair are differentiated in the elevational zones
115 they occupy (n=8 pairs). Bayesian linear models were used to assess differences in the
116 accumulation of selective sweeps with respect to divergence time, between the lowland-restricted
117 and elevationally-differentiated species pairs [25].

118 In light of evolutionary theory and natural history of the Amazon basin, we hypothesized
119 that glacial cycles in the mid- to late-Pleistocene drove selective sweeps in birds of the
120 Amazonian lowlands and highlands. More specifically, we hypothesized that the accumulation of
121 selective sweeps between sister species pairs over time would depend on their status as
122 elevationally differentiated or elevationally similar species. We predict that both divergent and
123 parallel selection would lead to an accumulation of selective sweeps over time between members
124 of a species pair. However, divergent selection would lead to a greater rate of selective sweep
125 accumulation than parallel selection as members of a newly diverged species pair adapted to
126 different environments.

127

128 **Methods**

129 *Study species*

130 We examined genomic divergence of 17 closely related allopatric species pairs: 9
131 lowland-restricted pairs, in which both species occur at low elevations in the Amazon basin; and
132 8 pairs at different elevations, in which one species belongs lower in the Amazonian lowlands
133 than the other in the Andean highlands. In the latter category, both species of the *Chlorospingus*
134 pair are Andean, but one occurring at higher elevations, *C. parvirostris*, than its sister species, *C.*
135 *flavigularis* (Supplementary Fig. S1). To explore the differences in elevation, we collated
136 elevational information for each species from either a book specializing in Amazonian birds [26]
137 when available, or the Birds of the World online resource if not [27–34]. At least four individuals
138 per species were analyzed (mean = 9.5; range = 4 to 24). Divergence time of species pairs spans
139 from 0.7 Ma to about 6 Ma, representing different stages of the speciation continuum.

140 Blood or tissue samples of most bird species from the tropical Andes were collected in
141 the Manu Biosphere Reserve in the Department of Cusco or at a variety of locations in the
142 Department of San Martín, Peru. Samples of lowland-restricted species were mostly obtained
143 from Matto Grosso, Brazil. Complementary tissue samples were obtained from Museu Paraense
144 Emilio Goeldi (MPEG), the Louisiana State University Museum of Natural Science (LSUMNS),
145 and the Field Museum of Natural History (FMNH).

146 *Library preparation and sequence data*

147 A total of 323 individuals were analyzed among 34 species (17 species pairs). DNA was
148 extracted from blood or tissue samples using E.N.Z.A tissue or blood extraction kits (Omega
149 Bio-Tek). Genotyping-By-Sequencing (GBS) libraries [35] were generated for all samples. The
150 Cornell Institute of Genomic Diversity generated libraries for several lowland species in the
151 dataset and these were sequenced on the Illumina HiSeq 2000 platform using 100 bp single-end
152 sequencing. An almost identical GBS method (following the protocol modifications in
153 Luzuriaga-Aveiga *et al.* 2021) was used to generate libraries for the remaining species. The latter
154 were sequenced on the Illumina HiSeq 4000 platform by the Centre for Applied Genomics at the
155 Hospital for Sick Children (SickKids), using 100 bp paired-end sequencing. Sequences of some
156 individuals have already been published by the Weir Lab. Details of individuals used, accession
157 numbers, and sequencing method can be found in the Supporting Online Materials.

158 Sequences were demultiplexed and filtered using the function *process_radtags* of the
159 STACKS 2.3 pipeline [37], with default parameters. Reads were trimmed for adapters and low-
160 quality sequences using Trimmomatric-0.38 [38], with the following parameters: TRAILING:3
161 SLIDINGWINDOW:4:10 MINLEN:30. Sequence reads of individuals of each species were
162 aligned to the reference genome of its closest relative available (Supporting Online Materials)

163 using Bowtie2: --phred33 --very-sensitive --mp 5,1 --score-min L, -0.6, -0.6. The *mpileup* and
164 *call* functions of BCFtools 1.12 [39] was used to call genotypes using default settings. Individual
165 genotype calls with < 5x depth and with a genotype likelihood of < 20 were set to missing.

166 For each species pair we generated three different filtered datasets, each used for different
167 purposes. Dataset 1 was used to calculate d_{XY} and π, for which variable and non-variable sites
168 are needed. We excluded sites with more than 90% missing genotype calls and SNPs with high
169 heterozygosity (>0.75). Dataset 2 was used to calculate F_{ST}, for which only biallelic sites are
170 required. SNPs with a minimum of 4 genotype calls per population were retained. We excluded
171 sites with minor allele frequency <0.05, with mean sequencing depth greater than 95th
172 percentile, and with observed heterozygosity exceeding 0.75. Dataset 3 was used to generate Site
173 Frequency Spectra (SFS). We used identical filtering parameters as in dataset 1, except we
174 removed genotype calls with < 10x depth, and to reduce linkage disequilibrium, we thinned
175 dataset 3 to retain only one SNP per 10 kb.

176 *Detection of lineage-specific selective sweeps*

177 We first ran a relatedness analysis of individuals within species, using *ngsRelate* [40].
178 For this analysis, we used unfiltered VCF files of all individuals per species and kept default
179 parameters for the estimation of Jacquard coefficients and relatedness summary statistics.
180 Individuals with co-ancestry coefficient (theta) > 0.1, equivalent to half sibling relationship or
181 higher [41] one of the two related individuals was removed.

182 Next, we examined signatures of selective sweeps in each of the 17 species pairs, using
183 summary statistics. We used Pixy 1.2.7 [42] to calculate $d_{XY,}$ using Dataset 1, and F_{ST} and π,
184 using Dataset 2, across 250 kb non-overlapping windows. Only windows with a minimum of 10

185 SNPs were retained. The female *W*-chromosome was excluded because many individuals were
186 male and we did not have enough female individuals in many comparisons to include the *W*. F_{ST},
187 d_{XY} and π for each window were transformed into *z*-scores by subtracting the mean across
188 windows and then dividing it by the standard deviation across windows. Mean and standard
189 deviations were calculated separately for each macrochromosome (chromosomes > 2.5-6 μm
190 long [43]; chromosomes 1-10, 1A, 4A and Z) and jointly for the microchromosomes
191 (chromosomes < 2.5 μm long; chromosomes 11- 29). One tailed *P*-values were calculated from
192 *z*-scores using the *pnorm* function in R [44], with lower.tail = FALSE to detect significant peaks
193 of F_{ST}, and lower.tail = TRUE to detect significant drops of π and d_{XY}. Peaks or drops were
194 considered significant if their *p*-value was ≤ 0.05.

195 Windows were considered to exhibit signatures consistent with lineage-specific selective
196 sweeps if they possessed significantly elevated peaks in F_{ST} and significantly reduced drops in π
197 in one (lineage-specific sweeps) or both (sweeps targeting the same window in both species)
198 species of a pair, and with no significant drop in d_{XY}. In contrast, a simultaneous drop in d_{XY}
199 (Fig. 2D) together with elevated in F_{ST} and π in both species of a pair would be consistent with
200 either a selective sweep that occurred in the common ancestor or of a selective sweep that
201 crossed species boundaries through introgression [45]. Selective sweep signatures may span
202 more than one 250 Kb window. To avoid counting these as multiple sweeps, we combined
203 windows of selection less than 1 Mb apart as a single sweep. We standardized the number of
204 detected selective sweeps across species pairs by dividing the number of windows of selection
205 observed by the total number of windows assessed per species pair.

206 *Estimation of divergence times*

207 We used FASTSIMCOAL2 [24] to estimate the effective population size (N_e) of each
208 member of a species pair, as well as divergence time from a common ancestor. We used
209 Arlequin v3.5 [46] to generate a multidimensional site frequency spectrum (SFS) of species by
210 re-filtering SNPs from down-samples of at least 4 (diploid) individuals per species. We used a
211 minimum site depth cutoff of 10 per individual and manually entered the number of non-variable
212 sites into the SFS. We used family-specific generation times found in the literature to calibrate
213 both per generation mutation rates, calculated from whole-genome datasets in Feng *et al.* (2020)
214 and time of divergence in Myr (Supplementary Table S1). These mutation rates were used to
215 calibrate our demographic models. To build an understanding of the data, we explored a linear
216 model of $\log_{10}N_e$ and mean π in a species, with the expectation that the two values should be
217 correlated.

218 *Patterns of adaptive genomic evolution through time*

219 Using linear regression, we compared how the number of detected selective sweeps
220 accumulated through time for species pairs restricted to the lowlands versus different elevations.
221 If elevational differentiation promotes divergent selection, we would expect to find a higher
222 number of selective sweeps and *y*-intercept (or slope) values in species pairs that occur at
223 different elevations versus lowland-restricted pairs. Potential phylogenetic non-independence of
224 sister pairs was corrected using the following approach. We pruned a time-calibrated phylogeny
225 of all birds of the world [48] to retain only one representative species for each pair in the dataset,
226 using the *keep.tip* function in the R package APE [49]. A phylogenetic multilevel model with the
227 number of detected sweeps dependent on the interaction of divergence time of each pair and
228 category (lowland versus different elevations), and the phylogenetic variance-covariance matrix

229 as a varying intercept was fit in the R package brms [25,50,51]. Specifically, we used a normal
230 distribution to fit the model, with normally distributed priors of mean 0 and standard deviation
231 0.01 for the model intercept and coefficients, and Student t-distributed priors with 3 degrees of
232 freedom for overall standard deviation and sigma. The model was run over 4 independent
233 Hamiltonian Monte Carlo chains, using 5,000 burn-in and 15,000 sampling iterations each
234 (60,000 iterations total). Adapt delta was raised to 0.999, and maximum tree depth was raised to
235 12. Trace lots, potential scale reduction factors $\hat{R}$ of 1, and posterior predictive checks over 100
236 draws were used to assess model fit. To assess differences between species pairs in the lowlands
237 versus those from different elevations, we used the *hypothesis* function in brms. Specifically, we
238 tested for three differences in brms:

239 1. To assess whether elevationally differentiated or lowland-restricted species pairs
240 had a greater rate of accumulation of selective sweeps over time, we tested
241 whether the slope of elevationally differentiated species pairs was greater than
242 the slope of lowland-restricted species pairs.

243 2. To assess the number of selective sweeps at different times due to species pairs
244 being elevationally differentiated or lowland-restricted, we tested whether the
245 number of observed selective sweeps was higher in the birds from different
246 elevations than lowland-restricted birds at 0.7, 2, 3, 4, and 5 Myr. The time at 0.7
247 Myr was approximately at the start of the mid- to late-Pleistocene glacial cycles.

248 3. To assess whether there were more selective sweeps in the lowlands-restricted
249 species pairs than the elevationally differentiated species pairs extrapolated to the
250 present day, we tested whether the intercept of the lowland-restricted species

251 pairs was higher than the intercept of the elevationally-differentiated species
252 pairs.

253 In addition, we used linear modeling to assess the possibility that other patterns may have
254 driven the observed selective sweeps, as opposed to ecologically-driven parallel or divergent
255 selection. Using linear models in R, we tested models of the number of detected sweeps
256 dependent on an interaction of either mean π or $\log_{10}N_e$ and elevational category at a species-
257 level, highland or lowland. Another linear model was used to assess whether the accumulation of
258 selective sweeps in highland-lowland pairs was driven by suboscine or oscine species. This was
259 done in a manner consistent with the overall model of selective sweeps and divergence time in
260 brms, except only lowland-highland species pairs were used, and a categorical variable of
261 suboscine or oscine was tested in its interaction with divergence time, rather than elevational
262 category, as previously done. Here, a directional hypothesis test was used to assess whether the
263 suboscine and oscine species each accumulated sweeps over time at a slope greater than 0, as we
264 predicted for the species pairs representing different elevations. We also visualized the
265 proportion of overlap in elevational ranges between lowlands-restricted species pairs and those
266 from different elevations, and plotted those values against the number of observed selective
267 sweeps.

268

269 **Results**

270 The species categorized as from highland elevations had generally greater elevational
271 ranges than lowland species (Supplementary Fig. S2). Two species pairs in genera
272 *Chlorospingus* and *Ramphocelus* had substantial overlap in elevational ranges between the low

273 and high elevation species in these pairs, but the populations studied nevertheless appear to be
274 elevational replacements where they co-occur on the same mountain slopes [26].

275 The standardized number of detected selective sweeps varied between species pairs and
276 elevational categories in a model with overall R^2 of 0.65 (95% credible interval (CI): [0.34,
277 0.88]) (Fig. 3). Lowland-restricted pairs had a flat relationship between detected selective sweeps
278 and age of the species pair (slope = 8.20×10^{-5}, 95% CI: [-1.62×10^{-3}, 1.52×10^{-3}]) while the pairs
279 from differing elevations had a strong positive increase (slope = 3.14×10^{-3}, 95% CI: [7.69×10^{-4},
280 5.31×10^{-3}]). An evidence ratio of 155.66 from a directional hypothesis test corresponded to a
281 99.4% posterior probability that the pairs from differing elevations had a higher slope than the
282 lowland-restricted pairs. In a test for whether the slope for lowland-restricted birds was > 0, the
283 evidence ratio was 0.83 and posterior probability was 45.5%, thus we could not distinguish this
284 slope from 0. The third and final use of the *hypothesis* function in brms showed that lowland-
285 restricted species pairs had more observed selective sweeps until approximately 2 Myr (evidence
286 ratio 12.09, posterior probability 92.4%), where the number of selective sweeps was
287 indistinguishable between the lowland-restricted and elevationally-differentiated pairs (evidence
288 ratio 1.02, posterior probability 50.4%), while beyond 2 Myr in the past, the elevationally-
289 differentiated pairs had more observed selective sweeps (evidence ratios of 19.48, 91.31, and
290 143.93 and posterior probabilities of 95.1%, 98.9%, and 99.3% at 3, 4, and 5 Myr respectively).
291 The lowland-restricted species pairs had a higher intercept than the elevationally differentiated
292 species pairs (evidence ratio 23.77, posterior probability 96.0%).

293 Observed π or N_e were correlated (r=0.72, adjusted R^2=0.50, p=2.01×10^{-6}; Supplementary
294 Fig. S3), and neither drove observations of selective sweeps, (p=0.17 and 0.40, respectively)
295 (Supplementary Figs. S4; S5). A paired t-test of pairs at different elevations shows that highland

species have consistently lower π but not $\log_{10}N_e$ relative to their lowland close relative (paired t-test: $p = 0.025$ (π), $p = 0.28$ (N_e); Fig. 4).

A limitation of our study design is the taxonomic mismatch between species categories. All species pairs from the Amazonian lowlands are suboscines, whereas species pairs at different elevations are phylogenetically more diverse, including two non-passerine pairs (motmots and woodpeckers), three oscines (tanagers and icterids) and three suboscines (woodcreepers, manakins, and flycatchers). However, we found that non-suboscine species in elevationally differentiated pairs accumulated selective sweeps at a similar pace through time as suboscine species, and both exhibited signatures of divergent selection as slopes were greater than 0 (oscine evidence ratio 44.6, 97.8% posterior probability; suboscine evidence ratio 381.2, 99.7% posterior probability) (Fig. S5). Moreover, all linear models were corrected for phylogenetic structure. As such, we do not believe that the differences in the patterns found here between lowland-restricted species pairs and pairs with elevation differentiation were driven by phylogenetic composition. In addition, no relationship was evident between the proportion of elevational range overlap and the number of selective sweeps in either category of lowlands-restricted species pairs or those from different elevations (Supplementary Fig. S7).

Discussion

Divergent selection is celebrated as a key driver of rapid evolutionary change, while the contribution of parallel selection is less well understood. Both have the potential to drive a rapid accumulation of selective sweeps. Here we quantified the number of selective sweep signatures accumulated through evolutionary time in related pairs of Amazonian species that differ greatly

318 in elevation and therefore likely experienced stronger divergent selection. We compared these
319 with pairs restricted to similar habitats at low elevations, which likely experienced weaker
320 divergent selection but are expected to have been strongly influenced by parallel selection
321 pressures. We found a substantially steeper increase in the number of selective sweeps through
322 time in elevationally differentiated pairs of species while species pairs at the same elevation
323 showed a flat relationship between sister species age and the number of observed selective
324 sweeps. This difference in slope was robust to phylogenetic structure, independent of genome-
325 wide π or N_e, and is consistent with the long-term effect of ecologically driven divergent
326 selection accelerating evolution over the course of millions of years in elevationally
327 differentiated pairs compared to lowland restricted pairs. Nevertheless, lowland restricted pairs
328 accumulated more selective sweeps over the glacial cycles of the past two million years, which
329 we suggest reflects the power of parallel selection to generate bursts of adaptation and genomic
330 evolution during periods of intense climate change.

331 For species pairs restricted to lowland regions, selective sweeps did not accumulate as a
332 function of time like they did in elevationally differentiated pairs. This observation would make
333 sense if the major climatic cycles of the past 700 kyr were overwhelmingly responsible for
334 selection compared to earlier periods. Under this scenario all species pairs from the same
335 lowland elevations older than 700 kyr (i.e., all species pairs in our dataset) should have
336 experienced roughly the same amount of selection, regardless of their differing time of
337 divergence from a common ancestor. These climatic cycles are believed to have caused a general
338 cooling and possibly decreased rainfall in lowland Amazonia [52,53]. Unlike highland species
339 which can track their preferred environments downslope during glacial periods, low elevation
340 species have nowhere to go, and are thus forced to adapt in parallel. Mid- to late-Pleistocene

341 climatic cycles would have thus intensified parallel selection pressures to adapt in lowland
342 species while the much more stable environment prior to these cycles would exert much weaker
343 selection. The flat relationship of our lowland restricted pairs between ~700 kyr and 5 Myr is
344 thus consistent with almost no detectable effect of selection prior to the glacial cycles, but a
345 substantial effect during them from ~700 kyr to the present. This contrasts with elevationally
346 differentiated pairs of species where the accumulation of selective sweeps through time is
347 strongly positive, suggesting ongoing divergent selection up to 5 Myr was driven by elevational
348 differentiation rather than just the effect of more recent Pleistocene glacial cycles.

349 In addition to the rate of selective sweep accumulation, the absolute number of observed
350 sweeps at different times was also informative for elucidating the roles for different types of
351 selection. There were more observed selective sweeps due to parallel than divergent selection
352 from the present up until approximately 2 Myr, after which there are more selective sweeps
353 attributable to divergent selection (Fig. 3). Therefore, while divergent selection had a consistent
354 effect over time and led to more selective sweeps in species pairs from different elevations,
355 parallel selection had a more prominent role in evolution during glacial cycles. This
356 interpretation relies on our assumption that species pairs at the same elevations experience
357 mostly parallel selection given the similar environments they are in. While environment is much
358 less variable across lowland Amazonia than it is along the elevational transects of the Andes,
359 some divergent selection driven by fine-scale spatial heterogeneity may have contributed to
360 selective sweeps in lowland-restricted species pairs [54] and our estimates cannot untangle the
361 contribution of these from the effect of parallel selection. Nevertheless, this finding challenges a
362 widespread belief that ecological and environmental differences accelerate speciation (i.e.,
363 ecological speciation) and are its key drivers, while parallel selection plays a less important role

364 in speciation [10]. Instead, our results suggest that parallel selection may be capable of driving
365 even faster evolutionary change when environments are unstable and species are forced to adapt
366 *in situ*.

367 Our methods are unlikely to capture all selective sweeps. First, adaptive alleles do not
368 always generate F_{ST} peaks when traits under selection are highly polygenic, because polygenic
369 traits may evolve with incomplete sweeps at many loci. In such cases, the influence of selection
370 on individual loci is likely too small to be detected [23]. Second, soft sweeps acting on standing
371 variation may generate too weak of a signature for our methods to detect, because with standing
372 variation the target of selection will have recombined with a variety of surrounding genetic
373 variants, which then fail to materialize as a sweep signature when the target is fixed (Fig. 2). It
374 thus remains possible that lowland-restricted species did experience selection before the mid- to
375 late-Pleistocene glacial cycles in primarily polygenic traits or soft sweeps. The stronger parallel
376 selection forces induced by the glacial cycles would then have driven an increase in hard sweep
377 signatures more recently which is the primary signal we detect. This scenario is also plausible
378 because greater nucleotide diversity observed in the lowland species (Supplementary Fig. S2)
379 means there is a larger pool of standing genetic variants present that soft selection could have
380 acted upon. Given these considerations, we can only conclude that our different patterns
381 uncovered between species pairs that do and do not have elevational differentiation primarily
382 reflect the effect of hard selective sweeps while the effect of soft sweeps and selection on highly
383 polygenic traits remains unknown.

384 Another limitation of this work is that genomic architecture may have influenced the
385 results. We analyzed F_{ST} and π in windows of at least 250 kb, thus, smaller sweeps may go
386 undetected and their detection will require whole genome sequencing. The larger sweeps we

387 were able to detect may be associated with architecture such as chromosomal inversions, which
388 are understood to support local adaptation and selective sweeps in a range of species [55,56].
389 Also, centromeres and telomeres possess low recombination rates that facilitate sweeps, which
390 lower π and elevate F_{ST} over broad genomic regions, thereby generating strong sweep signatures
391 that are easily detected (see Cutter & Payseur 2013). However, there are only a limited number
392 of these genomic features, and if they were a major contributor to our detections of selective
393 sweeps, the number of such selective sweep signatures we detected might accumulate rapidly
394 over short time scales and then remain constant with increasing time, as sweeps in older species
395 pairs would be overwritten by subsequent sweeps. In such a scenario, the elevationally-
396 differentiated pairs should also exhibit a flat relationship between species pair age and the
397 number of selective sweeps, like lowland-restricted pairs. Instead, we uncovered a strong
398 positive slope for elevationally-differentiated pairs (Fig. 3), indicating that avian genomes are
399 capable of accumulating detectable selective sweep signatures through time. Therefore, the
400 approach we adopted for detecting divergent selection might be influenced by, but was not
401 invalidated by, conserved genomic architecture.

402 In conclusion, despite the limitations of our approach, we found clear differences
403 between elevationally differentiated and lowland restricted species pairs in terms of selective
404 sweep accumulation through time. Over the five-million-year timescale of our dataset, strong
405 divergent selection associated with elevational differentiation resulted in a much greater number
406 of selective sweeps than seen in lowland restricted pairs, which confirms the importance of
407 divergent selection as has previously been emphasized (e.g., Schluter 2009). Nevertheless, our
408 data suggests lowland restricted species pairs accumulated more selective sweeps over the major
409 Pleistocene glacial cycles consistent with climate change forcing them to adapt *in situ*, while

410 highland species could track their preferred environment up and down slope with less need for
411 adaptation. Parallel selection may thus result in limited adaptation when environments are highly
412 constant through time (i.e., prior to major Pleistocene glacial cycles) but may elevate the rate of
413 accumulation of selective sweeps during periods of environmental instability (i.e., during major
414 Pleistocene glacial cycles) when parallel environmental changes force species to adapt. Parallel
415 selection is likely to target different genes in different populations, leading to genomic
416 differentiation and the accumulation of genetic incompatibilities that ultimately are believed to
417 play a key driving force in Amazonian speciation [57,58]. Our findings are consistent with a
418 recent meta-analysis of birds, mammals, reptiles, and other groups which found preliminary
419 evidence that parallel selection was a generally stronger force in shaping trait evolution than
420 divergent natural selection [14]. Together, these results suggest parallel selection may drive
421 adaptation and speciation during periods of intense environmental change in the most species
422 rich region of the planet. While the role of divergent natural selection has been well documented,
423 there remains a great need for studies to address the contribution of parallel selection to
424 adaptation and speciation.

425

426 **Acknowledgements**

427 Else Mikkelsen and Jordan Bemmels provided valuable discussions throughout this study. Ellen
428 Nikelski helped improve an earlier draft. Land-owners of Brazil graciously allowed us to sample
429 on their properties. Alexandre Alexio facilitated Brazilian collecting permits (Brazilian National
430 Research Council 4253-1, 40173-1 and 6581-1). Mauricio Ugarte-Lewis facilitated Peruvian
431 collecting permits (RDG N° 158–2017-SERFOR-DGGSPFFS). The following museums
432 provided tissue samples: Museu Paraense Emlio Goeldi, Louisiana Museum of Natural History,
433 and Field Museum of Natural History. Funding was supplied by the National Secretariat of
434 Science, Technology and Innovation (SENESCYT-IFTH) from Ecuador to V.E.L.A., the Eric

and Wendy Schmidt AI in Science Postdoctoral Fellowship, a program of Schmidt Sciences, LLC (to M.J.T.), and Natural Sciences and Engineering Research Council of Canada (NSERC) Discovery Grant RGPIN-2012-418294, RGPIN-2019-04260 (to J.E.J.) and National Science Foundation Grant DEB-1120682 (to J.E.J.), and the Natural Sciences and Engineering Research Council of Canada Accelerator Grant (no. 492890; to J.T.W.), Discovery Grants (402013-2011, RGPIN-2016-0653, RGPIN-2022-04817) to J.T.W.

Literature cited

1. Darwin C, Wallace A. 1858 On the Tendency of Species to form Varieties; and on the Perpetuation of Varieties and Species by Natural Means of Selection. *Journal of the Proceedings of the Linnean Society of London. Zoology* **3**, 45–62. (doi:10.1111/j.1096-3642.1858.tb02500.x)

2. Maan ME, Seehausen O. 2011 Ecology, sexual selection and speciation: Ecology, sexual selection and speciation. *Ecology Letters* **14**, 591–602. (doi:10.1111/j.1461-0248.2011.01606.x)

3. Ogden R, Thorpe RS. 2002 Molecular evidence for ecological speciation in tropical habitats. *Proceedings of the National Academy of Sciences* **99**, 13612–13615. (doi:10.1073/pnas.212248499)

4. Price T. 2008 *Speciation in birds*. Greenwood Village, Colo: Roberts and Co.

5. Schluter D. 2000 *The ecology of adaptive radiation*. Oxford: Oxford University Press.

6. Campagna L, Toews DPL. 2022 The genomics of adaptation in birds. *Current Biology* **32**, R1173–R1186. (doi:10.1016/j.cub.2022.07.076)

7. Nosil P, Funk DJ, Ortiz-Barrientos D. 2009 Divergent selection and heterogeneous genomic divergence. *Molecular Ecology* **18**, 375–402. (doi:10.1111/j.1365-294X.2008.03946.x)

8. Nosil P. 2012 *Ecological speciation*. Oxford ; New York: Oxford University Press.

9. Rundle HD, Nosil P. 2005 Ecological speciation: Ecological speciation. *Ecology Letters* **8**, 336–352. (doi:10.1111/j.1461-0248.2004.00715.x)

10. Schluter D. 2009 Evidence for Ecological Speciation and Its Alternative. *Science* **323**, 737–741. (doi:10.1126/science.1160006)

11. Cerca J. 2023 Understanding natural selection and similarity: Convergent, parallel and repeated evolution. *Molecular Ecology* **32**, 5451–5462. (doi:10.1111/mec.17132)

12. Mani GS, Clarke BC. 1990 Mutational Order: A Major Stochastic Process in Evolution. *Proceedings of the Royal Society of London. Series B, Biological Sciences* **240**, 29–37.

13. Nosil P, Flaxman SM. 2011 Conditions for mutation-order speciation. *Proc. R. Soc. B* **278**, 399–407. (doi:10.1098/rspb.2010.1215)

14. Anderson SAS, Weir JT. 2022 The role of divergent ecological adaptation during allopatric speciation in vertebrates. *Science* **378**, 1214–1218. (doi:10.1126/science.abo7719)

15. Ridgely RS, Greenfield PJ. 2001 *The birds of Ecuador*. Ithaca, NY: Comstock Pub.

16. Smith BT *et al.* 2014 The drivers of tropical speciation. *Nature* **515**, 406–409. (doi:10.1038/nature13687)

17. Hooghiemstra H. 1989 Quaternary and upper-pliocene glaciations and forest development in the tropical andes: Evidence from a long high-resolution pollen record from the sedimentary basin of Bogotá, Colombia. *Palaeogeography, Palaeoclimatology, Palaeoecology* **72**, 11–26. (doi:10.1016/0031-0182(89)90129-6)

18. Hooghiemstra H, Melice JL, Berger A, Shackleton NJ. 1993 Frequency spectra and paleoclimatic variability of the high-resolution 30–1450 ka Funza I pollen record (Eastern Cordillera, Colombia). *Quaternary Science Reviews* **12**, 141–156. (doi:10.1016/0277-3791(93)90013-C)

19. Hooghiemstra H, Van Der Hammen T. 2004 Quaternary Ice-Age dynamics in the Colombian Andes: developing an understanding of our legacy. *Phil. Trans. R. Soc. Lond. B* **359**, 173–181. (doi:10.1098/rstb.2003.1420)

20. Wolf JBW, Ellegren H. 2017 Making sense of genomic islands of differentiation in light of speciation. *Nat Rev Genet* **18**, 87–100. (doi:10.1038/nrg.2016.133)

21. Boitard S, Schlotterer C, Nolte V, Pandey RV, Futschik A. 2012 Detecting Selective Sweeps from Pooled Next-Generation Sequencing Samples. *Molecular Biology and Evolution* **29**, 2177–2186. (doi:10.1093/molbev/mss090)

22. Hejase HA, Salman-Minkov A, Campagna L, Hubisz MJ, Lovette IJ, Gronau I, Siepel A. 2020 Genomic islands of differentiation in a rapid avian radiation have been driven by recent selective sweeps. *Proc Natl Acad Sci USA* **117**, 30554–30565. (doi:10.1073/pnas.2015987117)

23. Stephan W. 2016 Signatures of positive selection: from selective sweeps at individual loci to subtle allele frequency changes in polygenic adaptation. *Mol Ecol* **25**, 79–88. (doi:10.1111/mec.13288)

24. Excoffier L, Foll M. 2011 fastsimcoal: a continuous-time coalescent simulator of genomic diversity under arbitrarily complex evolutionary scenarios. *Bioinformatics* **27**, 1332–1334. (doi:10.1093/bioinformatics/btr124)

25. Bürkner P-C. 2021 Bayesian Item Response Modeling in *R* with **brms** and *Stan*. *J. Stat. Soft.* **100**. (doi:10.18637/jss.v100.i05)

26. Schulenberg TS, Stotz DF, Lane DF, O'Neill JP, Parker III TA. 2007 *Birds of Peru*. 1st edn. Princeton, New Jersey: Princeton University Press.

27. Del Hoyo J, Collar N, Kirwan GM, Sharpe C. 2020 Rondonia Warbling-Antbird (Hypocnemis ochrogyna). In *Birds of the World* (eds SM Billerman, BK Keeney, PG Rodewald, TS Schulenberg), Cornell Lab of Ornithology. (doi:10.2173/bow.ronwaa1.01)

28. Del Hoyo J, Collar N, Kirwan GM. 2020 Spix's Warbling-Antbird (Hypocnemis striata). In *Birds of the World* (eds SM Billerman, BK Keeney, PG Rodewald, TS Schulenberg), Cornell Lab of Ornithology. (doi:10.2173/bow.spiwaa1.01)

29. Marantz CA, Aleixo A, Bevier LR, Patten MA. 2020 Spix's Woodcreeper (Xiphorhynchus spixii). In *Birds of the World* (eds SM Billerman, BK Keeney, PG Rodewald, TS Schulenberg), Cornell Lab of Ornithology. (doi:10.2173/bow.spiwoo1.01)

30. Snow D. 2020 Red-headed Manakin (Ceratopipra rubrocapilla). In *Birds of the World* (eds SM Billerman, BK Keeney, PG Rodewald, TS Schulenberg), Cornell Lab of Ornithology. (doi:10.2173/bow.rehman1.01)

31. Snow D. 2020 Crimson-hooded Manakin (Pipra aureola). In *Birds of the World* (eds SM Billerman, BK Keeney, PG Rodewald, TS Schulenberg), Cornell Lab of Ornithology. (doi:10.2173/bow.crhman1.01)

32. Snow D, De Juana E. 2020 Snow-capped Manakin (Lepidothrix nattereri). In *Birds of the World* (eds SM Billerman, BK Keeney, PG Rodewald, TS Schulenberg), Cornell Lab of Ornithology. (doi:10.2173/bow.sncman1.01)

33. Snow D, Sharpe C. 2020 Opal-crowned Manakin (Lepidothrix iris). In *Birds of the World* (eds SM Billerman, BK Keeney, PG Rodewald, TS Schulenberg), Cornell Lab of Ornithology. (doi:10.2173/bow.opcman1.01)

34. Zimmer K, Isler ML, De Juana E. 2020 Silvered Antbird (Sclateria naevia). In *Birds of the World* (eds SM Billerman, BK Keeney, PG Rodewald, TS Schulenberg), Cornell Lab of Ornithology. (doi:10.2173/bow.silant1.01)

35. Elshire RJ, Glaubitz JC, Sun Q, Poland JA, Kawamoto K, Buckler ES, Mitchell SE. 2011 A Robust, Simple Genotyping-by-Sequencing (GBS) Approach for High Diversity Species. *PLoS ONE* **6**, e19379. (doi:10.1371/journal.pone.0019379)

36. Luzuriaga-Aveiga V, Ugarte M, Weir JT. 2021 Distinguishing genomic homogenization from parapatric speciation in an elevationally replacing pair of *Ramphocelus* tanagers. *Mol Ecol* **30**, 5517–5529. (doi:10.1111/mec.16128)

37. Catchen JM, Amores A, Hohenlohe P, Cresko W, Postlethwait JH. 2011 *Stacks* : Building and Genotyping Loci *De Novo* From Short-Read Sequences. *G3 Genes|Genomes|Genetics* **1**, 171–182. (doi:10.1534/g3.111.000240)

38. Bolger AM, Lohse M, Usadel B. 2014 Trimmomatic: a flexible trimmer for Illumina sequence data. *Bioinformatics* **30**, 2114–2120. (doi:10.1093/bioinformatics/btu170)

39. Li H. 2011 A statistical framework for SNP calling, mutation discovery, association mapping and population genetical parameter estimation from sequencing data. *Bioinformatics* **27**, 2987–2993. (doi:10.1093/bioinformatics/btr509)

40. Korneliussen TS, Moltke I. 2015 NgsRelate: a software tool for estimating pairwise relatedness from next-generation sequencing data. *Bioinformatics* , btv509. (doi:10.1093/bioinformatics/btv509)

41. Ackerman MS, Johri P, Spitze K, Xu S, Doak TG, Young K, Lynch M. 2017 Estimating Seven Coefficients of Pairwise Relatedness Using Population-Genomic Data. *Genetics* **206**, 105–118. (doi:10.1534/genetics.116.190660)

42. Korunes KL, Samuk K. 2021 PIXY : Unbiased estimation of nucleotide diversity and divergence in the presence of missing data. *Molecular Ecology Resources* **21**, 1359–1368. (doi:10.1111/1755-0998.13326)

43. Griffin DK, Robertson LBW, Tempest HG, Skinner BM. 2007 The evolution of the avian genome as revealed by comparative molecular cytogenetics. *Cytogenet Genome Res* **117**, 64–77. (doi:10.1159/000103166)

44. R Core Team. 2021 R: A language and environment for statistical computing.

45. Irwin DE, Alcaide M, Delmore KE, Irwin JH, Owens GL. 2016 Recurrent selection explains parallel evolution of genomic regions of high relative but low absolute differentiation in a ring species. *Mol Ecol* **25**, 4488–4507. (doi:10.1111/mec.13792)

46. Excoffier L, Lischer HEL. 2010 Arlequin suite ver 3.5: a new series of programs to perform population genetics analyses under Linux and Windows. *Molecular Ecology Resources* **10**, 564–567. (doi:10.1111/j.1755-0998.2010.02847.x)

47. Feng S *et al.* 2020 Dense sampling of bird diversity increases power of comparative genomics. *Nature* **587**, 252–257. (doi:10.1038/s41586-020-2873-9)

48. Pulido-Santacruz P, Weir JT. 2016 Extinction as a driver of avian latitudinal diversity gradients: EXTINCTION AS A DRIVER OF DIVERSITY GRADIENTS. *Evolution* **70**, 860–872. (doi:10.1111/evo.12899)

49. Paradis E, Schliep K. 2019 ape 5.0: an environment for modern phylogenetics and evolutionary analyses in R. *Bioinformatics* **35**, 526–528. (doi:10.1093/bioinformatics/bty633)

50. Bürkner P-C. 2017 **brms** : An *R* Package for Bayesian Multilevel Models Using *Stan*. *J. Stat. Soft.* **80**. (doi:10.18637/jss.v080.i01)

51. Bürkner P-C. 2018 Advanced Bayesian Multilevel Modeling with the R Package brms. *The R Journal* **10**, 395. (doi:10.32614/RJ-2018-017)

52. Ramírez-Barahona S, Eguiarte LE. 2013 The role of glacial cycles in promoting genetic diversity in the Neotropics: the case of cloud forests during the Last Glacial Maximum. *Ecol Evol* **3**, 725–738. (doi:10.1002/ece3.483)

53. Rull V. 2011 Neotropical biodiversity: timing and potential drivers. *Trends in Ecology & Evolution* **26**, 508–513. (doi:10.1016/j.tree.2011.05.011)

54. Michot V, Corpetti T, Ronchail J, Espinoza JC, Arvor D, Funatsu BM, Dubreuil V. 2024 Seasonal types in homogeneous rainfall regions of the Amazon basin. *Intl Journal of Climatology* **44**, 1224–1244. (doi:10.1002/joc.8380)

55. Cutter AD, Payseur BA. 2013 Genomic signatures of selection at linked sites: unifying the disparity among species. *Nat Rev Genet* **14**, 262–274. (doi:10.1038/nrg3425)

56. Wellenreuther M, Bernatchez L. 2018 Eco-Evolutionary Genomics of Chromosomal Inversions. *Trends in Ecology & Evolution* **33**, 427–440. (doi:10.1016/j.tree.2018.04.002)

57. Cronemberger ÁA, Aleixo A, Mikkelsen EK, Weir JT. 2020 Postzygotic isolation drives genomic speciation between highly cryptic *Hypocnemis* antbirds from Amazonia. *Evolution* **74**, 2512–2525. (doi:10.1111/evo.14103)

58. Pulido-Santacruz P, Aleixo A, Weir JT. 2018 Morphologically cryptic Amazonian bird species pairs exhibit strong postzygotic reproductive isolation. *Proc. R. Soc. B.* **285**, 20172081. (doi:10.1098/rspb.2017.2081)

Tables & Figures

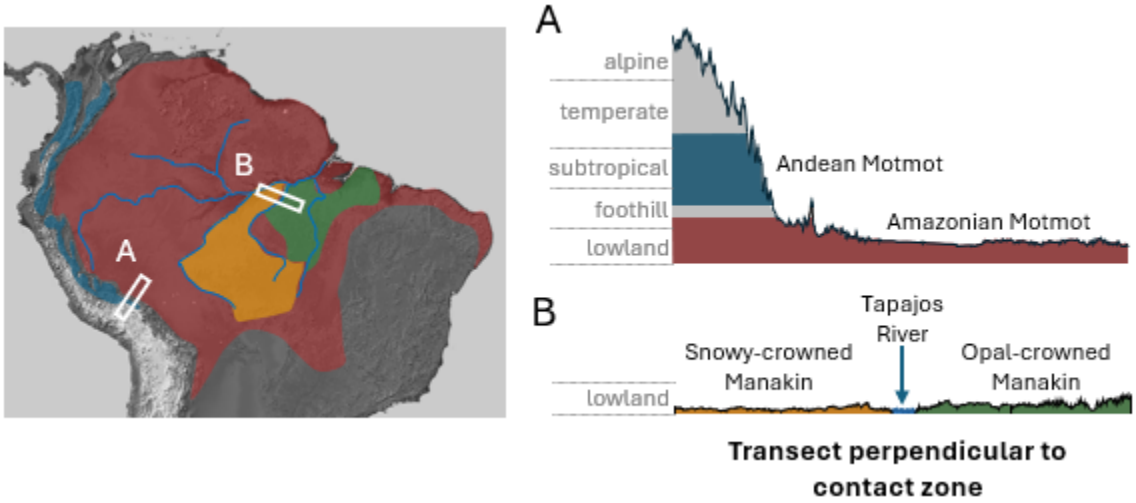

Figure 1. Geographic ranges of two example species pairs overlaid on a topographical map of South America. In A) the foothill forest zone occurs from approximately 600 to 1,300 m (foothill), the epiphyte encrusted subtropical montane forest zone from approximately 1,300 to 2,400 m (subtropical), the temperate montane forest zone to the treeline at approximately 3,300 m (temperate), and the alpine zone exists above 3,300 m. One species pair has the Amazonian Motmot (*Momotus momota*), in red, distributed in lowland forest from 0 to 700 m and its sister species, the Andean Motmot (*M. aequatorialis*), in blue, distributed in Andean cloud forest from 1000 to 2300 m. The other species pair has both species distributed in low elevation rainforest in different regions of the Amazon basin, with the Opal-crowed Manakin *(Lepidothrix iris*) distributed east of the Tapajos River and the Snowy-crowed Manakin (*L. nattereri*) distributed west of the river. Insets A and B show 250 km-long transects running perpendicular to the contact zones between each species pair. Coloured bands show the elevational profiles of each species. Shaded relief topographical base map obtained from NASA (https://www.nasa.gov). Major rivers of the Amazon basin are shown in blue.

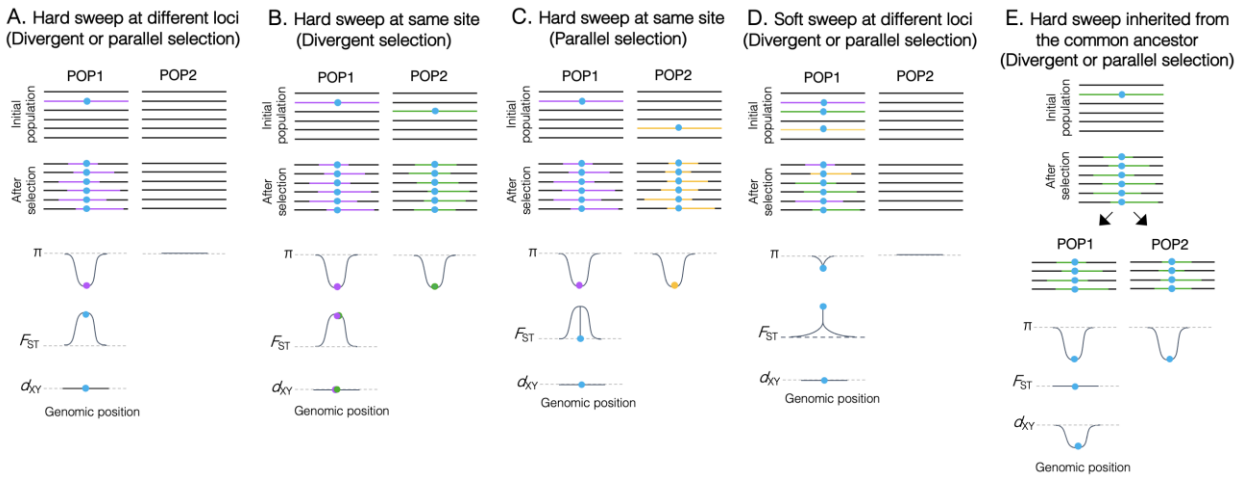

Figure 2. Hard and soft selective sweeps, with corresponding expectations of π, F_{ST} and d_{XY} under divergent and parallel selection. In hard sweeps (A–C, E), a positively selected de novo mutation (turquoise circle) arises in a single genomic background. Selection causes fixation of this mutation together with closely linked surrounding blocks of the genomic background that have not had time to experience recombination (coloured segments). The soft sweep (D) is similar, but the allele that is the target of selection is segregating in the population prior to becoming positively selected, resulting in all genomic backgrounds it is associated with increasing in frequency. The resulting patterns of π, F_{ST} and d_{XY} after selection can be used to detect potential selective sweeps. Hard sweeps at different loci (A) result in drops in π only in the species that is the target of selection for a given locus. The drop in π elevates F_{ST}. Hard sweeps at the same site (B–C) result in a drop in π in both species and an increase in F_{ST}. They produce almost identical patterns of F_{ST} and π under divergent (B) and parallel (C) selection but differ only in the value of F_{ST} at the site that is the target of selection, with the site having an F_{ST} of 1 under divergent selection (where different alleles at the site of selection are fixed), and an F_{ST} of 0 under parallel selection (where the same allele at the site of selection is fixed). Sweeps resulting from divergent or parallel selection cannot easily be discriminated. Soft sweeps at different loci (D) produce similar patterns in π and F_{ST} as hard sweeps, but the drops in π and increases in F_{ST} are less extreme, making them harder to detect. A sweep in the common ancestor of two populations (E) should result in both daughter populations inheriting low π around the selected site, but, unlike sweeps at the same site in both populations, an ancestral sweep results in a drop in F_{ST} and in d_{XY} between the daughter populations. Turquoise circles show the allele that is the target of selection. Coloured lines represent different haplotype blocks.

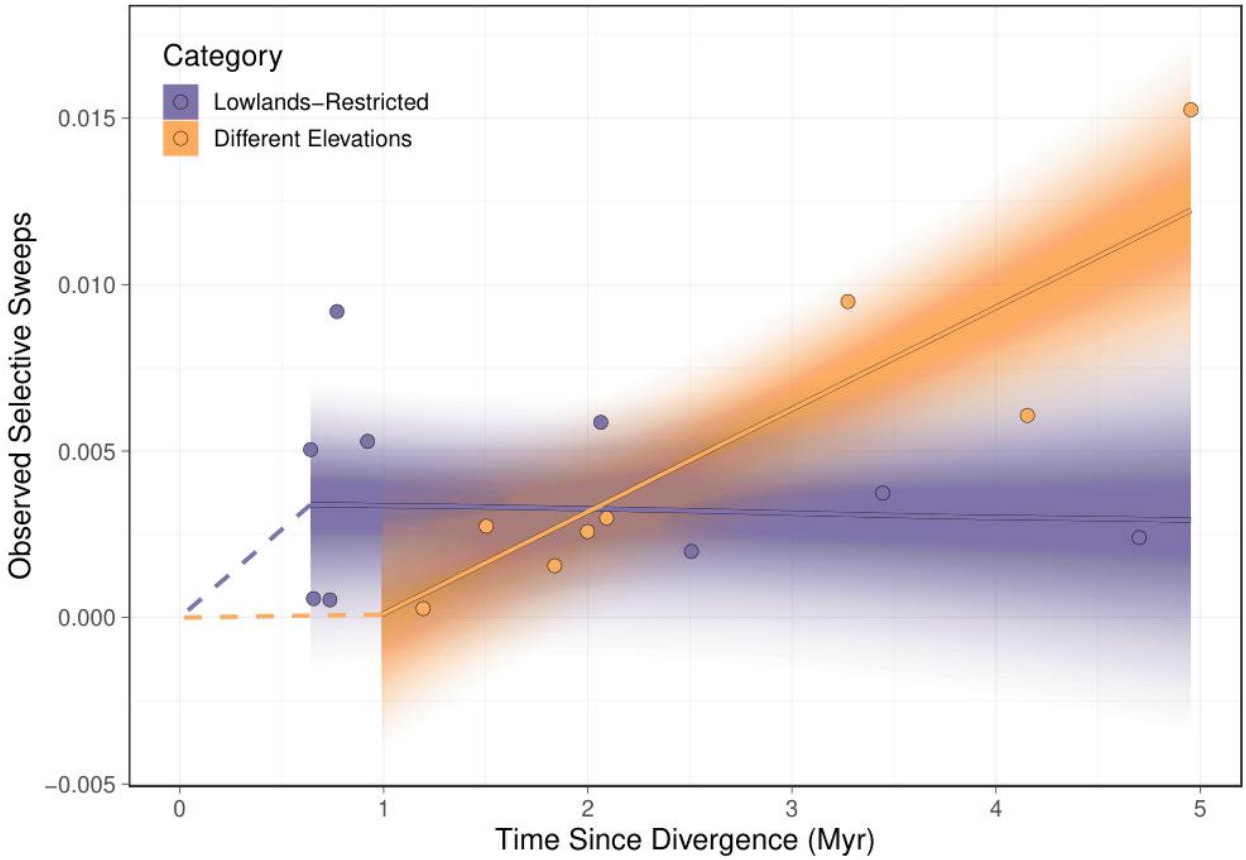

Figure 3. Number of observed selective sweeps accumulated between species pairs versus their divergence times, calculated from the nuclear genome using demographic modeling. Species pairs restricted to the Amazonian lowlands are shown with purple, and pairs occupying different elevational zones from the Amazonian lowlands towards the high Andes are shown in orange. Lines show model fits with phylogenetic relatedness accounted for. The lightest shading shows 95% credible intervals, while darker shading shows 10% credible intervals to emphasize posterior distributions underlying estimates of this linear model. Dashed lines reach from the most recent estimate of each line to the present day of 0 Myr, to emphasize selective sweep accumulation in the mid- to late-Pleistocene.

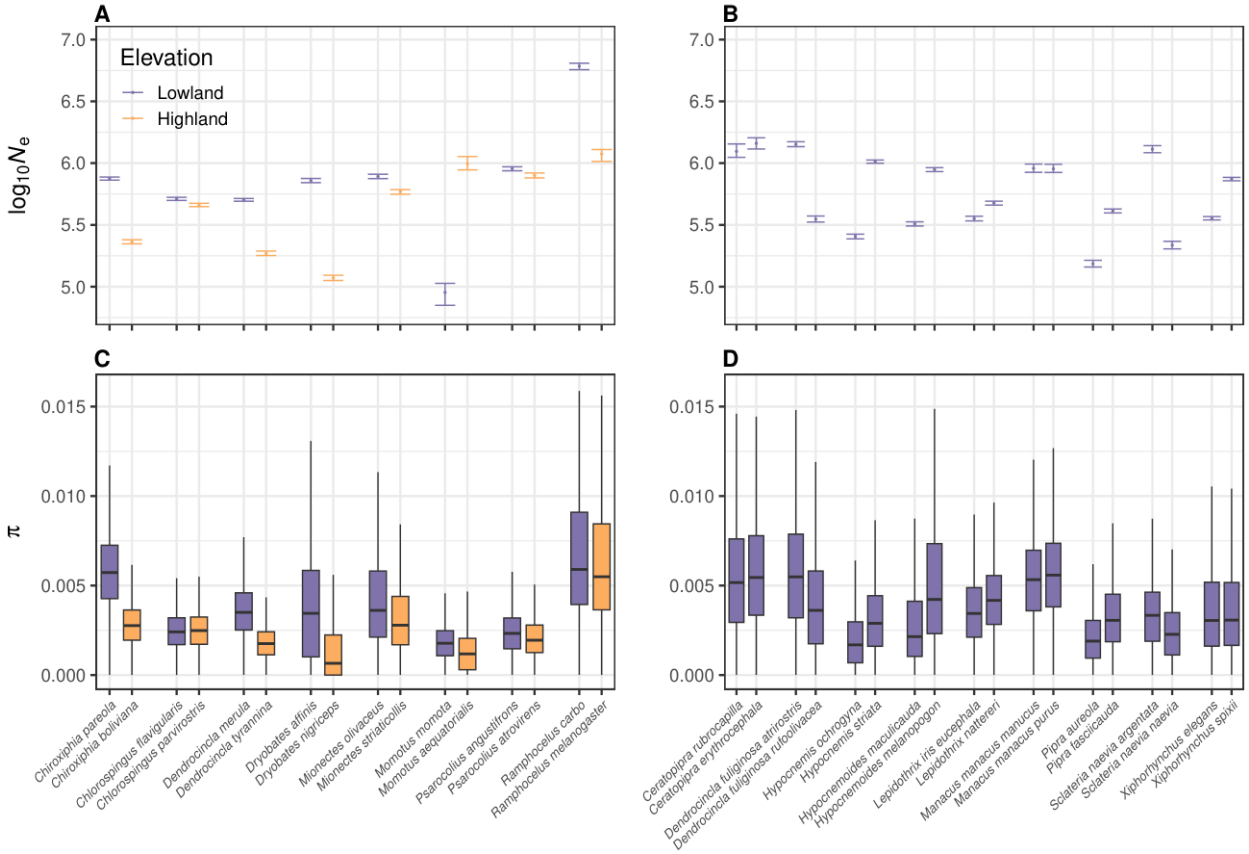

Figure 4. Estimated effective population size ($\log_{10}N_e$, top panels A and B) and box and whisker plots of average genome-wide nucleotide diversity (mean π, bottom panels C and D) across 250 Kb genomic windows. Species delineated by category, between pairs from different elevations (A and C) and lowland-restricted pairs (B and D). Lowland species are in purple, while highland species are in orange.

Supporting Information

Supplementary Table S1: Generation times and mutation rates used in coalescent modelling for major families represented in the dataset.

Family	Genus	Generation time	Mutation rate
Icteridae	*Psarocolius*	Mean = 1.83	2.096×10^{-9}
Thraupidae	*Ramphocelus*	Mean = 2.86	3.98×10^{-9}
Passerellidae	*Chlorospingus*	Mean = 2.33	2.99×10^{-9}
Thamnophilidae	*Hypocnemoides* *Hypocnemis* *Sclateria*	Mean = 2.44	4.14×10^{-9}
Dendrocolaptidae	*Xiphorhynchus* *Dendrocincla*	Mean = 2.83	4.14×10^{-9}
Tyrannidae	*Mionectes*	Mean = 1.98	3.73×10^{-9}
Pipridae	*Ceratopipra* *Pipra* *Lepidothrix* *Manacus* *Chiroxiphia*	Mean = 3.34	6.06×10^{-9}
Picidae	*Dryobates*	Mean = 2.86	6.89×10^{-9}
Momotidae	*Momotus*	Mean = 2.85	5.84×10^{-9}

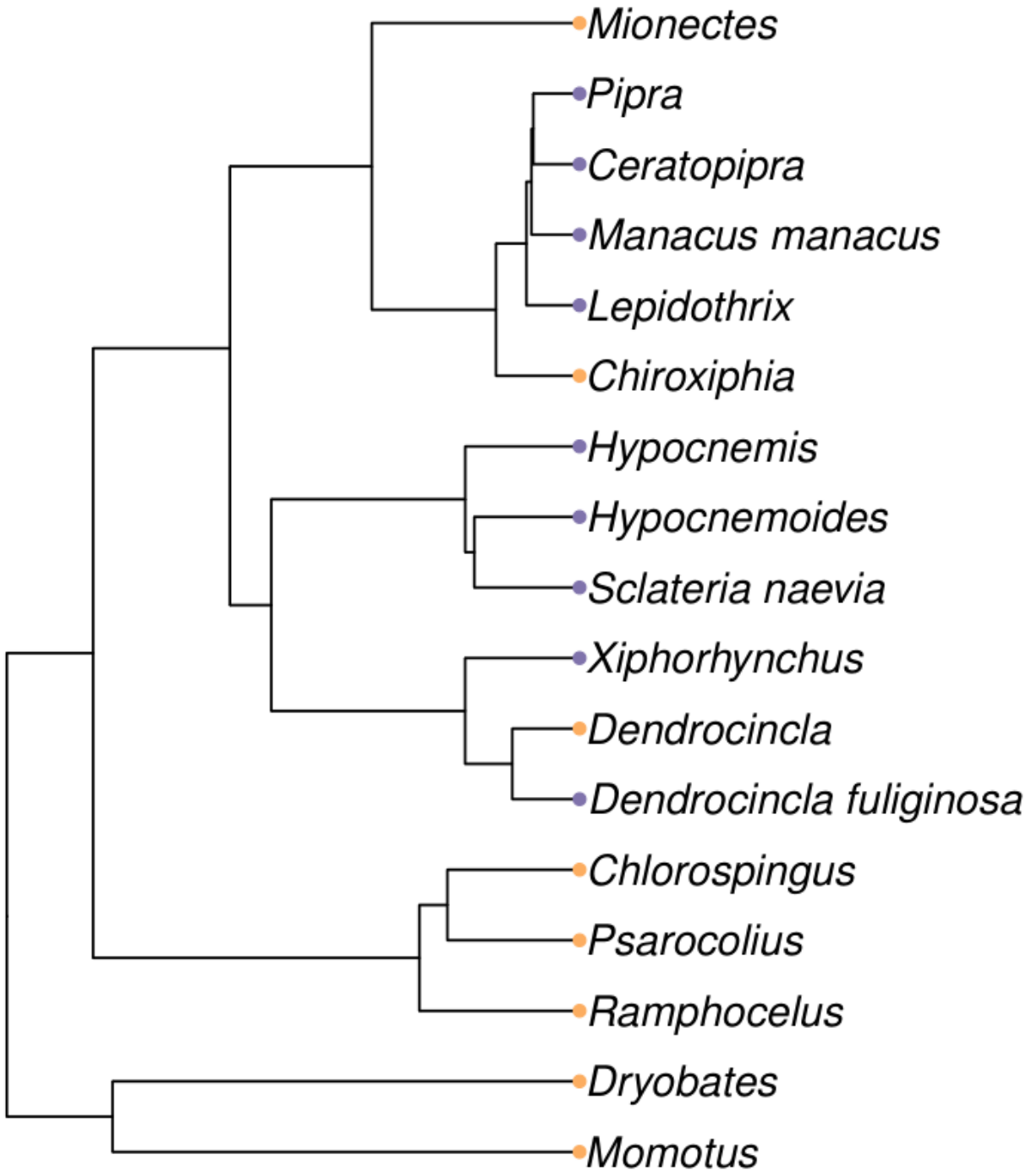

Figure S1. Phylogeny of the taxa included in the dataset. Tips of the tree represent sister species or subspecies pairs, colour-coded by their elevational category: purple for lowland-restricted pairs and orange for pairs at different elevations. *Dendrocincla fuliginosa* from the lowlands represents two subspecies, *D. f. atrirostris* and *D. f. rufoolivacea*. *Dendrocincla* at different elevations represents *D. merula* and *D. tyrannina.*

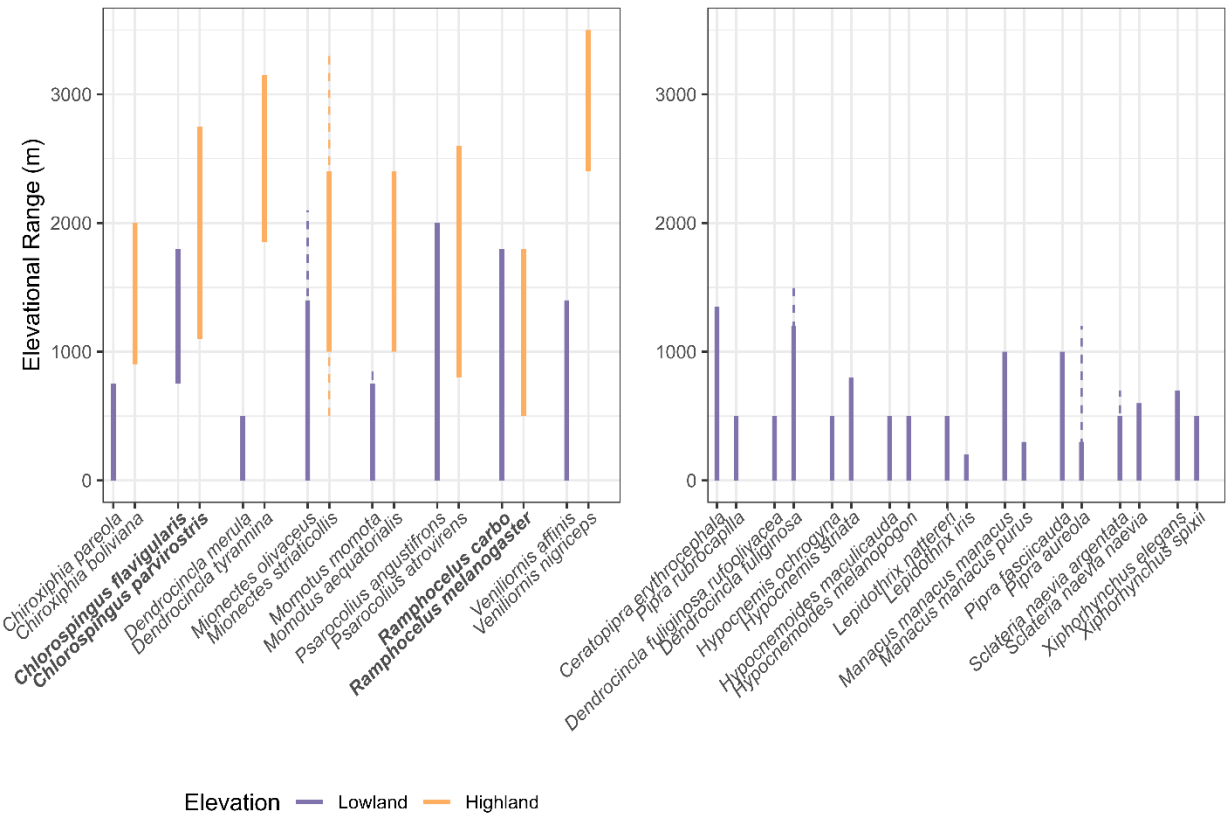

Figure S2. Elevational ranges for species in the present study. For species where both a core range and maximum and minimum observations were recorded, dashed lines were used to show the extreme ends of a range. However, this information was not available consistently. While genera *Chlorospingus* and *Ramphocelus* (bold) had largely overlapping species elevational ranges, they were allopatric and likely experienced different historical environments.

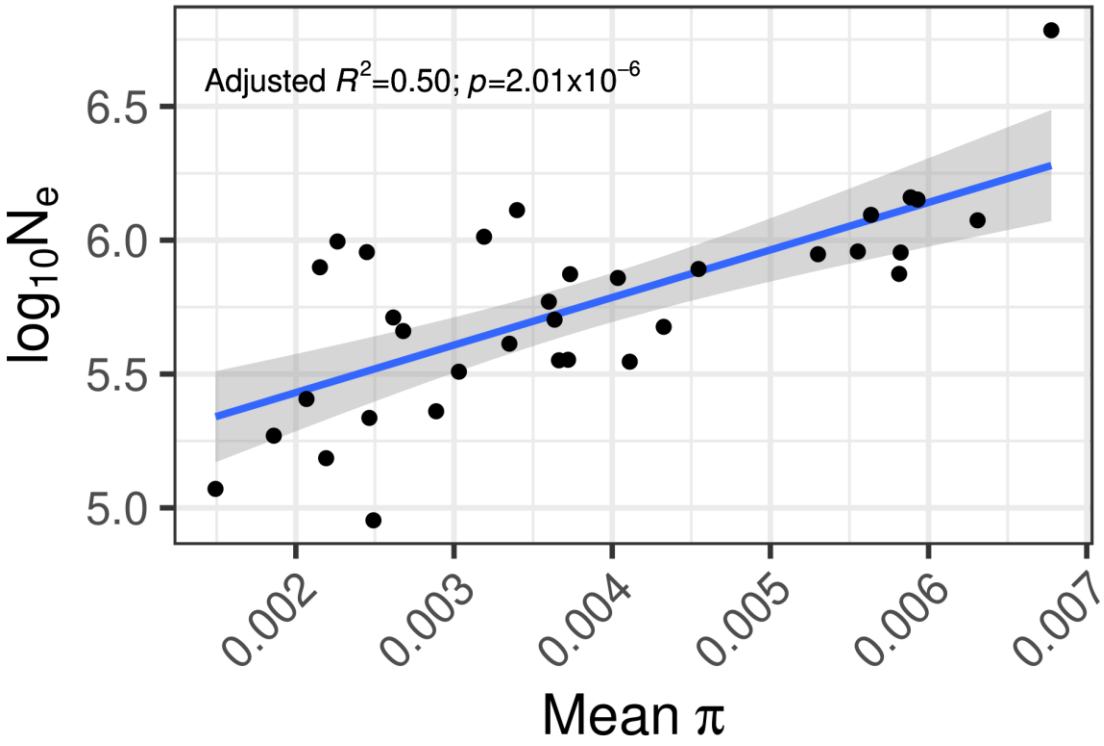

Figure S3. Linear regression between effective population size (N_e) and mean genome-wide nucleotide diversity (π).

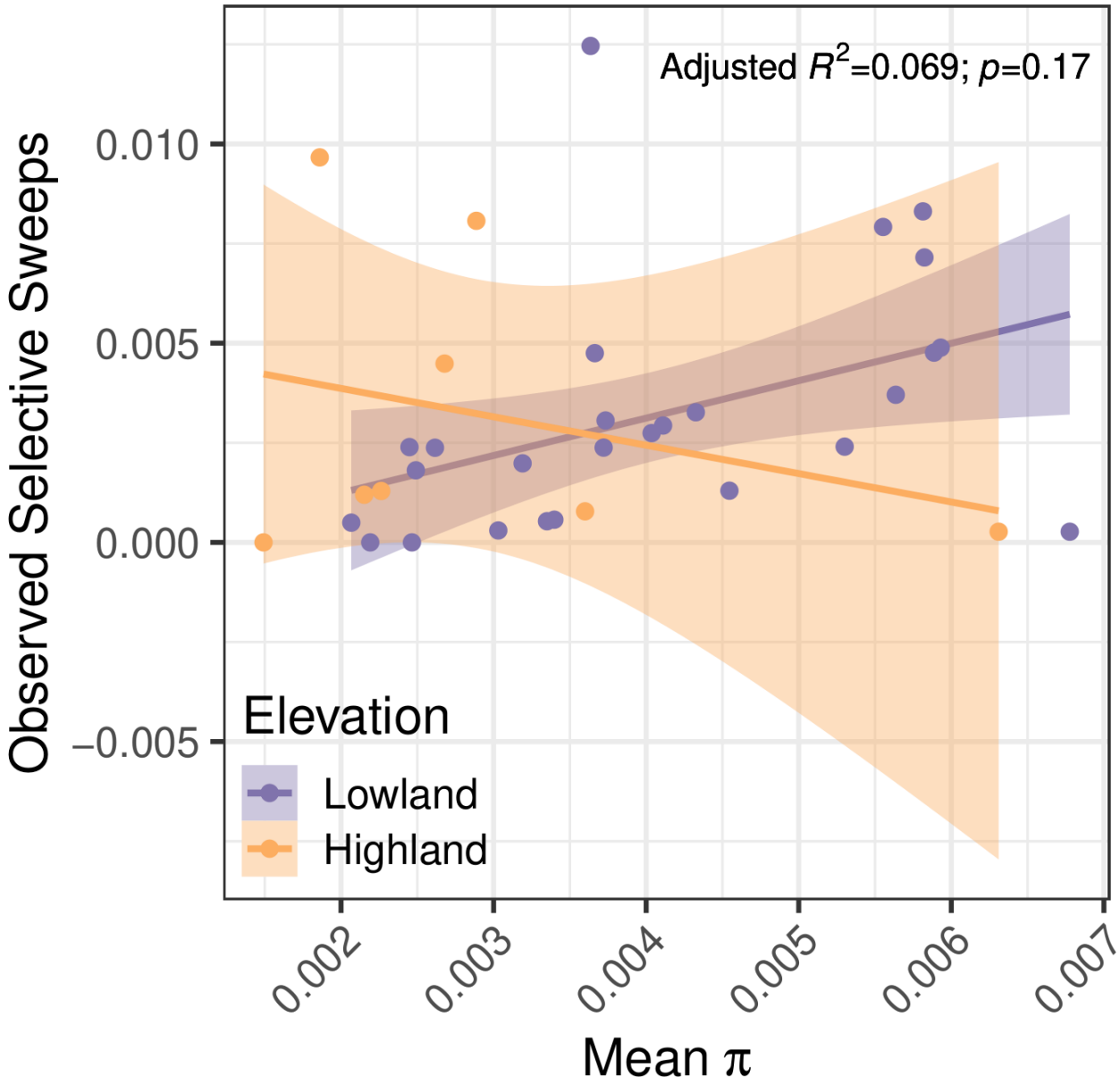

Figure S4. Regression analyses between number of lineage-specific windows of selection and average genome-wide nucleotide diversity, π, for individual species (not species pairs). Here, mean π interacted with elevational category of lowland or highland. Species from the Andean highlands are shown in orange, and lowland Amazonian species are shown in purple. This model was not significant (p=0.17).

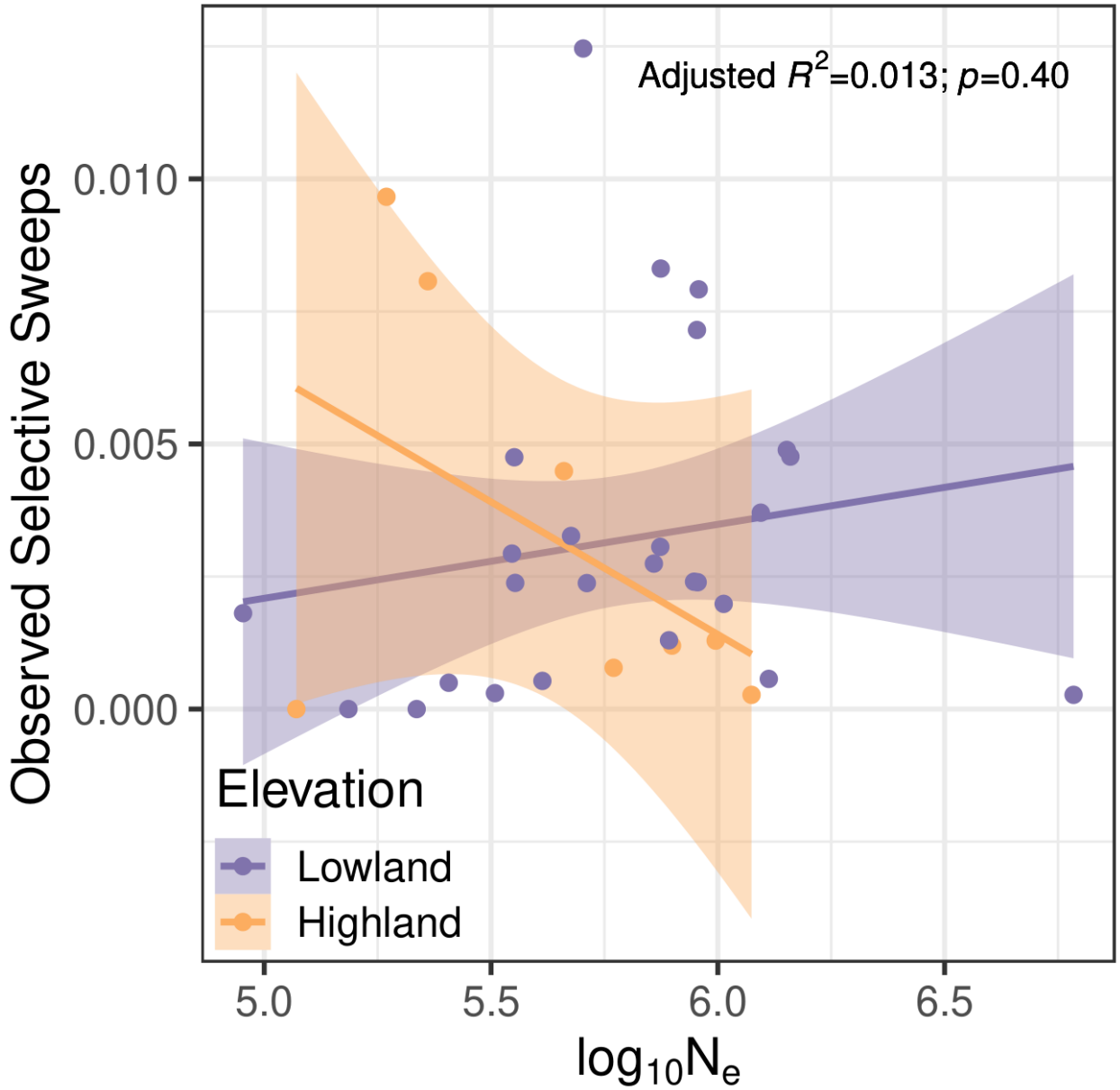

Figure S5. Regression analyses between the number of lineage-specific windows of selection and $\log_{10}$ effective population size ($\log_{10}N_e$) for individual species. Here, $\log_{10}N_e$ interacted with elevational category of lowland or highland. Species from the Andean highlands are shown in orange, and lowland Amazonian species are shown in purple. This model was not significant (p=0.40).

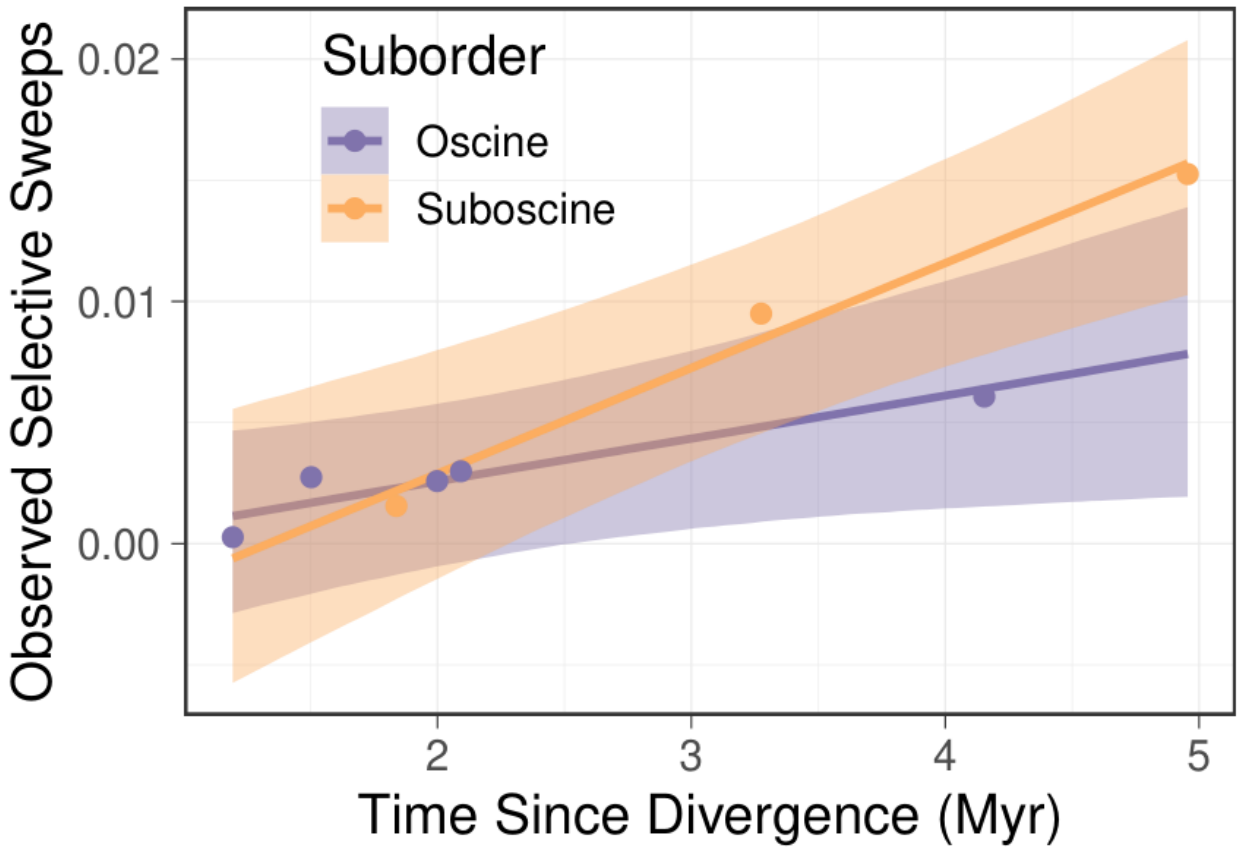

Figure S6. Number of observed selective sweeps accumulated between species pairs versus their divergence times, calculated from the nuclear genome using demographic modeling for only elevationally differentiated species pairs. Oscine species pairs are shown in purple, and suboscine pairs are shown in orange. Lines show model fits with phylogenetic relatedness accounted for. Shading shows the 95% credible intervals.

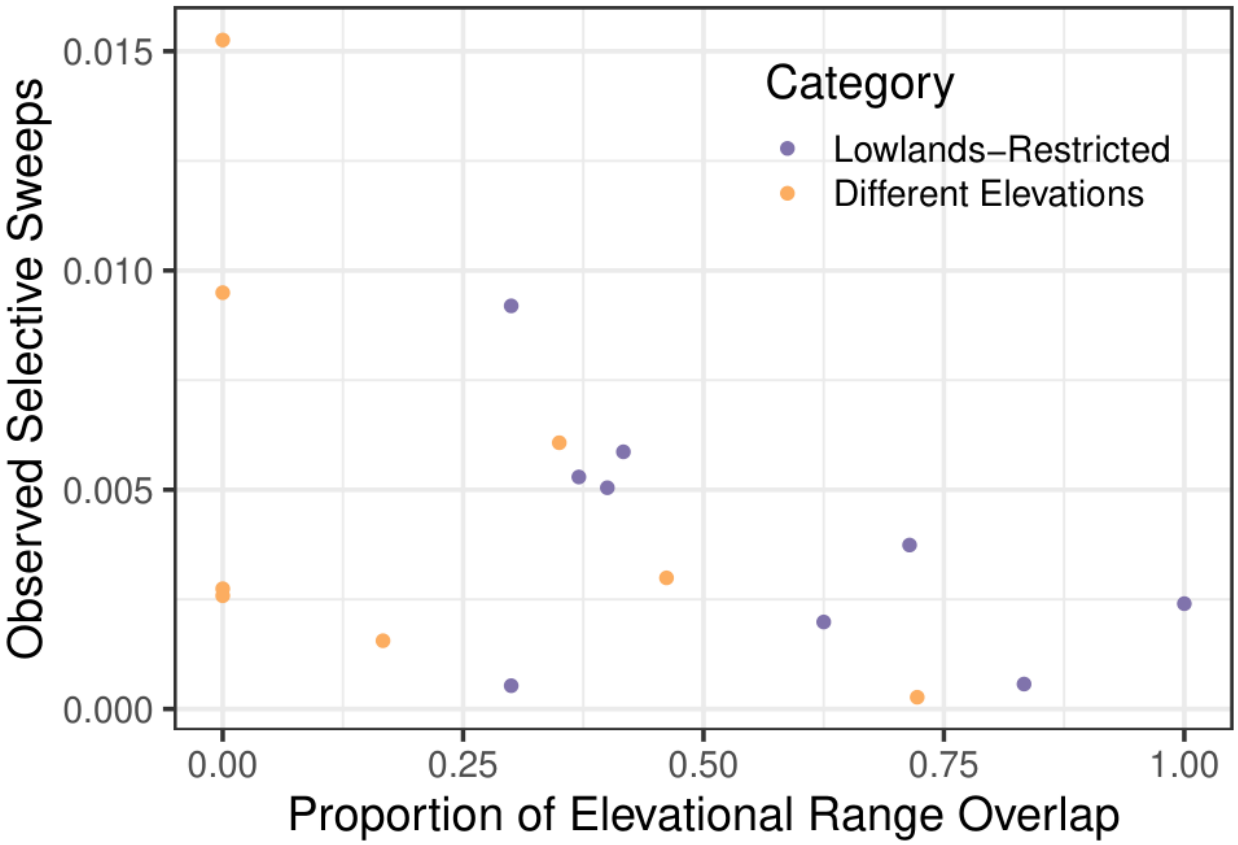

Figure S7. Proportion of elevational range overlap for each sister species pair, within lowlands-restricted or different elevation categories, against observed selective sweeps.

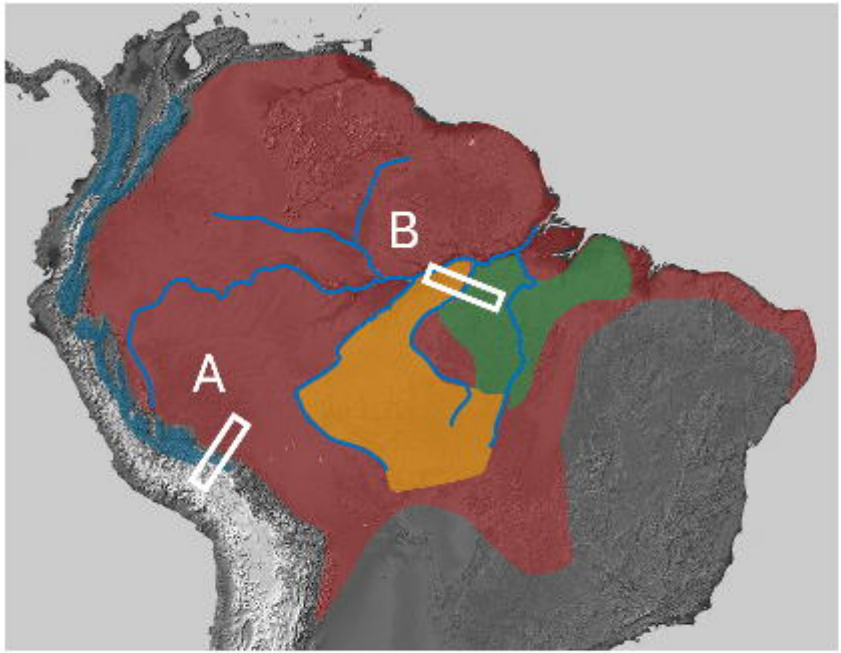

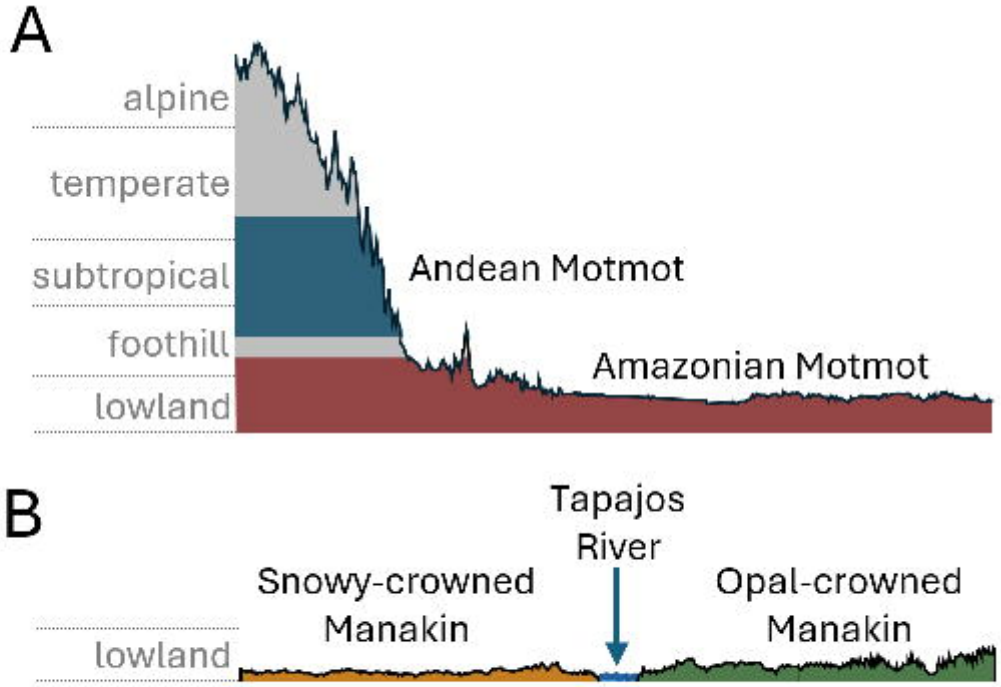

Transect perpendicular to contact zone

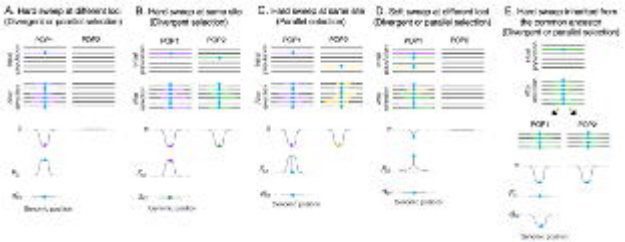
A. Hard sweep at different loci
(Divergent or parallel selection)
B. Hard sweep at same site
(Divergent selection)
C. Hard sweep at same site
(Parallel selection)
D. Soft sweep at different loci
(Divergent or parallel selection)
E. Hard sweep inherited from the common ancestor
(Divergent or parallel selection)
POP1
POP2
Selected position

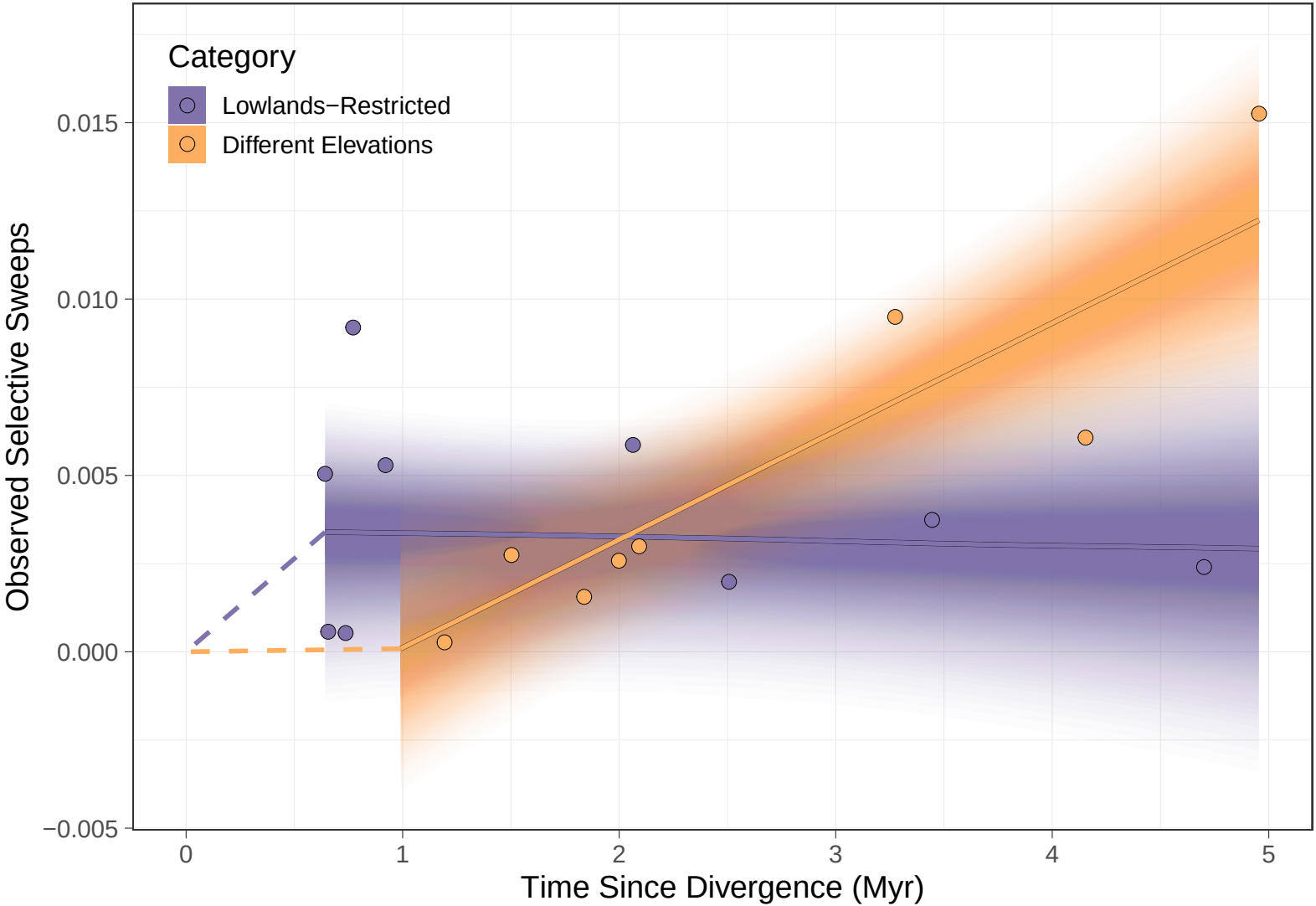
Category
Lowlands−Restricted
Different Elevations
Observed Selective Sweeps
0.015
0.010
0.005
0.000
−0.005
0
1
2
3
4
5
Time Since Divergence (Myr)

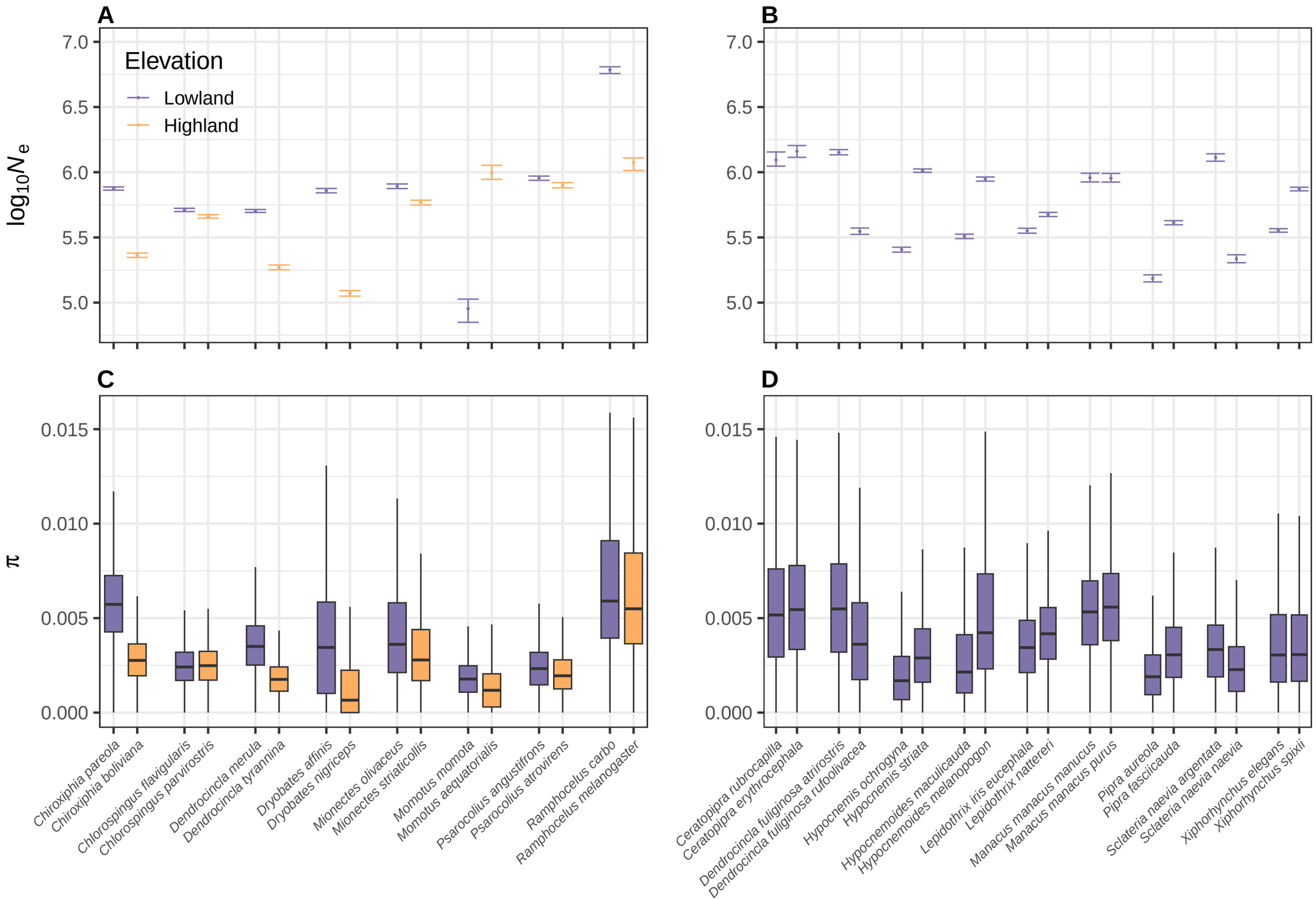
A
B
C
D
Elevation
Lowland
Highland
$\log_{10}N_e$
π
7.0
6.5
6.0
5.5
5.0
0.015
0.010
0.005
0.000
Chiroxiphia pareola
Chiroxiphia boliviana
Chlorospingus flavigularis
Chlorospingus parvirostris
Dendrocincla merula
Dendrocincla tyrannina
Dryobates affinis
Dryobates nigriceps
Mionectes olivaceus
Mionectes striaticollis
Momotus momota
Momotus aequatorialis
Psarocolius angustifrons
Psarocolius atrovirens
Ramphocelus carbo
Ramphocelus melanogaster
Ceratopipra rubrocapilla
Ceratopipra erythrocephala
Dendrocincla fuliginosa atrirostris
Dendrocincla fuliginosa rufoolivacea
Hypocnemis ochrogyna
Hypocnemis striata
Hypocnemoides maculicauda
Hypocnemoides melanopogon
Lepidothrix iris eucephala
Lepidothrix nattereri
Manacus manacus manucus
Manacus manacus purus
Pipra aureola
Pipra fasciicauda
Sclateria naevia argentata
Sclateria naevia naevia
Xiphorhynchus elegans
Xiphorhynchus spixii